Available online at www.CivileJournal.org

Civil Engineering Journal

(E-ISSN: 2476-3055; ISSN: 2676-6957)

Vol. 11, No. 09, September, 2025

Behavior of Full-Scale One-Way Semi-Precast Concrete Slabs with Varying Sizes and Shear Connectors

Kadhim Z. Naser [1*], Hussein A. Al-Gusab [1], Ansam Z. Thamer [1], Abdulamir A. Almayah [1], Muthana Sh. Mahdi [1], Mazin D. Abdullah [1]

[1] *Department of Civil Engineering, College of Engineering, University of Basrah, Basrah 61004, Iraq.*

Received 27 June 2025; Revised 11 August 2025; Accepted 17 August 2025; Published 01 September 2025

Abstract

This study investigates the structural performance of semi-precast concrete slabs (SPCSs), an innovative hybrid construction system that integrates factory-produced precast concrete units with a cast-in-place (CIP) concrete topping to create a composite structural element. This system offers notable advantages in terms of construction acceleration, improved quality control, and reduced labor requirements, as the precast unit serves as both a load-bearing component and a permanent formwork. To evaluate the structural behavior of the SPCSs, an experimental program was conducted on seven full-scale, one-way slab specimens with varying span lengths (4.75 m and 6.0 m), precast unit thicknesses (80 mm and 100 mm), and shear connector geometries (rectangular and triangular). A control slab without shear connectors was also tested to establish a baseline for comparison. The results demonstrated that the inclusion of shear connectors significantly enhanced structural performance. Specifically, the ultimate load capacity increased by 186.4%, and the cracking load increased by 220% compared to the control specimen. Rectangular connectors proved more effective than triangular ones in minimizing interface slip and enhancing ductility. The initial stiffness increased by 163.95%, while the energy dissipation capacity improved by 411.35%. Although variations in span length and topping thickness had relatively minor effects, the presence and geometry of shear connectors played a decisive role in ensuring effective composite action. All reinforced slabs exhibited flexural failure modes, indicating strong bonding and interaction between the precast and cast-in-place (CIP) concrete layers, whereas the control slab experienced premature failure due to interlayer debonding. Theoretical equations based on ACI 318-19 were used to estimate the nominal flexural capacities of the hybrid SPCS slabs, showing reliable agreement with the experimental results. These findings demonstrated the importance of shear connector design in maximizing the load-bearing capacity, ductility, and structural stiffness of SPCS systems under both service and extreme loading conditions.

Keywords: Full Scale; Semi-Precast Concrete Slabs; Composite Action; Shear Connectors; One-Way Slabs; Cast-In-Place Concrete; Shear Connector Shapes; Energy; Dissipation Interface Slip.

1. Introduction

Semi-precast concrete slabs (SPCS) represent a hybrid construction system that integrates precast concrete elements with a cast-in-place concrete (CIP) layer to form a composite structural unit. In this system, precast concrete slabs are manufactured off-site to serve as a base, upon which cast-in-place concrete is poured to complete the composite action. This approach combines the precision, construction speed, and quality assurance associated with precast elements with the adaptability and economic advantages of traditional cast-in-place concrete. One of the most significant advantages

* Corresponding author: kadhim.naser@uobasrah.edu.iq

http://dx.doi.org/10.28991/CEJ-2025-011-09-07

of SPCS is reducing the reliance on temporary formwork, as precast units often serve as permanent formwork. This feature significantly streamlines the construction process, reducing labor requirements, lowering costs, and shortening project duration. Moreover, the off-site manufacture of precast components under controlled conditions ensures superior quality control and adherence to engineering specifications. The minimized use of timber formwork not only lowers material costs but also contributes to environmentally friendly construction practices. This synergy between efficiency, quality, and sustainability has led to the widespread adoption of precast concrete systems in various structural engineering applications [1-11].

A primary advantage of SPCS systems lies in their cost-efficiency and reduced construction time, largely attributable to the minimized requirements for on-site formwork. Previous research indicates that SPCS systems can reduce formwork costs by up to 40% [12-16] and enhance construction productivity by a factor of up to 1.7 compared to conventional cast-in-situ systems [17]. These efficiencies, coupled with environmental benefits such as reduced timber consumption and site waste, have led to their widespread use in many countries [18-23]. From a structural perspective, the performance of SPCS systems depends primarily on the composite interaction between the precast and cast-in-situ layers. This interaction directly influences key mechanical behaviors, including flexural strength, shear strength, deflection, and cracking behavior [24-28]. Maintaining strain compatibility under various loading conditions is largely dependent on adequate interfacial surface shear capacity, as highlighted by ACI Committee 318 (2019) [29]. Surface treatments, such as roughening, moisture control, and curing [30, 31], as well as the use of shear keys, significantly improve shear transfer [32]. Additionally, appropriate reinforcements, including dowels and truss girders, are vital for achieving full composite action [24–28]. Material compatibility, practically regarding differential shrinkage, must also be carefully managed to prevent residual stresses that could compromise long-term durability [32].

The flexural performance of semi-precast concrete slab systems is influenced by the material properties of both the precast and cast-in-place concrete layers, as well as the embedded reinforcement. These factors affect both instantaneous and long-term deflection behavior [31] and govern the stiffness of the composite section [33, 34]. Although composite slabs may achieve similar static performance to monolithic slabs, their dynamic behavior may require specific design considerations. In seismic applications, interface detailing and shear connector configuration are crucial for ensuring adequate stiffness, strength, and ductility [35–37].

Numerous studies have investigated the structural behavior of SPCS. For instance, Supriyadi et al. (2017) [35] conducted a comparative analysis of the static and dynamic responses between semi-precast and monolithic slabs. Their results indicated that while semi-precast slabs exhibited a slight decrease in stiffness and natural frequency, their load-bearing capacity remained comparable to those of monolithic slabs. The observed correlation between flexural behavior and crack patterns suggests the potential for developing effective analytical models for design optimization. Similarly, Mohammed et al. (2020) [30] performed full-scale experimental and numerical analyses on SPCS systems incorporating various surface treatments and topping concrete. Their research revealed that achieving an interface shear strength exceeding 1.0 MPa was sufficient for the slab to behave monolithically. They identified transverse roughening as the most cost-effective method for achieving the required shear strength. Furthermore, their validated finite element models indicated that temporary propping during construction might be necessary for longer spans.

Furthermore, Murtado (2017) [37] studied the flexural performance of curved semi-precast slabs using both finite element analysis (FEA) and the strip method. While the strip method slightly overestimated the strength, both methodologies demonstrated consistent stiffness. Furthermore, the appearance of flexural cracks in regions of high moment confirmed flexural failure as the governing mechanism. In a separate study, Hillebrand & Heeger (2023) [36] examined the shear behavior of semi-precast slabs incorporating truss girders under monotonic loading. Their results indicated that slabs with roughened interfaces and enhanced internal detailing outperformed current code predictions. Notably, even slabs with smooth interfaces exceeded expectations, thereby confirming the conservative nature of existing design guidelines. Saheed et al. (2020) [38] explored lightweight precast slabs incorporating expanded polystyrene (EPS) and quarry dust. Among 256 trail mixes, up to a 20% weight reduction was achieved with satisfactory strength levels. While the shear strength was marginally lower, results surpassed theoretical expectations, supporting their sustainable application.

Yun et al. (2022) [39] investigated truss-girder slab connections through seven full-span specimens, revealing that relocating lap splices away from the mid-span and employing keyed or helical joints significantly enhanced flexural strength. In particular, keyed joints achieved 110% of the performance of monolithic slabs, making them advantageous for long-span applications. Zajac et al. (2021) [40] examined the structural behavior of various precast slab configurations. While slabs with concrete-only joints offered limited redistribution, those with cast-in-place topping demonstrated enhanced lateral stiffness. Beam models were found to overestimate deflection, whereas joint-hinged finite element models (FEMs) provided more accurate predictions, highlighting the need for refined analytical modeling approaches. Recently, Cao et al. (2023) [41] developed a three-layer composite slab consisting of ultra-high-performance concrete (UHPC), expanded polystyrene (EPS), and normal concrete. Large-scale tests confirmed strong composite action, with UHPC significantly improving crack control and ductility. A modified stress model based on ACI 544.4R predicted flexural behavior with only 3.4% error, while UHPC increased the flexural strength of the EPS layer by 11.5%.

Construction efficiency was emphasized by Cho et al. (2017) [17], who found that half-precast concrete slab systems (HPCSS) achieved 1.7 times higher productivity than conventional systems, with formwork and reinforcement identified as critical labor inputs. Kim (2015) [42] investigated spiral joints in half-depth precast bridge decks, demonstrating that reducing reinforcement spacing increased ultimate strength by 1.52 times and improved crack control, validating their use for flexural continuity. Irawan et al. (2017) [34] proposed a two-way SPCS system with a rigid triangular joint. Despite slightly higher deflection than monolithic slabs, the system effectively transmitted biaxial moments without additional formwork, supporting its use in long-span applications. Szydlowski & Szreniawa (2017) [43] introduced a semi-precast slab system using prestressed slabs as permanent formwork and reinforcement. Their theoretical study showed promising flexural performance for 8-meter spans with a 200 mm thickness, though full-scale validation was recommended. Bozzo & Torres (2004) [44] developed a semi-prestressed composite slab system combining flat beams, precast prestressed slabs, and an in-situ layer. It allowed for composite action over 12 × 12 meter spans at only 300 mm depth, with minimal long-term deflection. Hassan et al. (2021) [45] presented interlocking steel-concrete connections that improved load capacity by 40% compared to non-composite systems, matching the behavior of continuous slabs.

Lee et al. (2016) [16] designed a semi-prestressed slab system combining pre- and post-tensioning. Their parametric analysis enhanced safety and constructability in accordance with ACI 318. Zając et al. (2020) [32] evaluated Teriva panels with shear keys, observing minimal displacement (≤1.0 mm) and no cracks, indicating strong inter-component interaction. Ha et al. (2014) [46] tested U-shaped column-beam connections under cyclic loads, showing that transverse reinforcement significantly enhanced seismic performance per ACI T1.1.01. Mokhtar et al. (2020) [47] studied hidden corbel connections and found that the BHC2 type offered high ductility, improved confinement, and qualified as semi-rigid under Zone III conditions.

Collectively, these studies confirm the structural viability and efficiency of semi-precast concrete systems, highlighting the critical role of connection details, prestressing techniques, and interface behavior in optimizing design and promoting broader adoption in modern construction.

2. Significance of the Study

Despite the growing body of research on semi-precast concrete slab systems, a critical research gap persists in the systematic understanding of their full-scale structural behavior under varying geometric and connection conditions. Most previous studies have been confined to small-scale experimental models or numerical simulations, often isolating individual parameters such as surface treatment or connector type. There is a clear deficiency in integrated experimental investigations that examine the combined effects of slab span, precast unit thickness, and shear connector geometry within realistic, full-scale one-way slab configurations. This gap is particularly significant given the increasing demand for structural systems that are both constructible and high-performing in terms of stiffness, ductility, and energy dissipation.

Addressing this gap is vital to advancing design practices and ensuring the reliable performance of SPCSs in actual construction settings. A deeper understanding of how connector details and slab dimensions interact to influence flexural behavior and composite materials will allow for better optimization of structural systems, especially in applications requiring long spans and rapid construction. Furthermore, enhanced experimental data will support the calibration of analytical models and future refinement of structural design codes. Accordingly, the present study aims to experimentally investigate the flexural behavior of full-scale one-way semi-precast concrete slabs with varying spans, precast concrete thicknesses, and shear connector shapes. The study focuses on evaluating load-bearing capacity, interface performance, post-cracking stiffness, and dominant failure modes, with the ultimate goal of providing practical insights to support safer and more efficient design of hybrid concrete slab systems. Figure 1 illustrates a schematic flowchart of the research methodology.

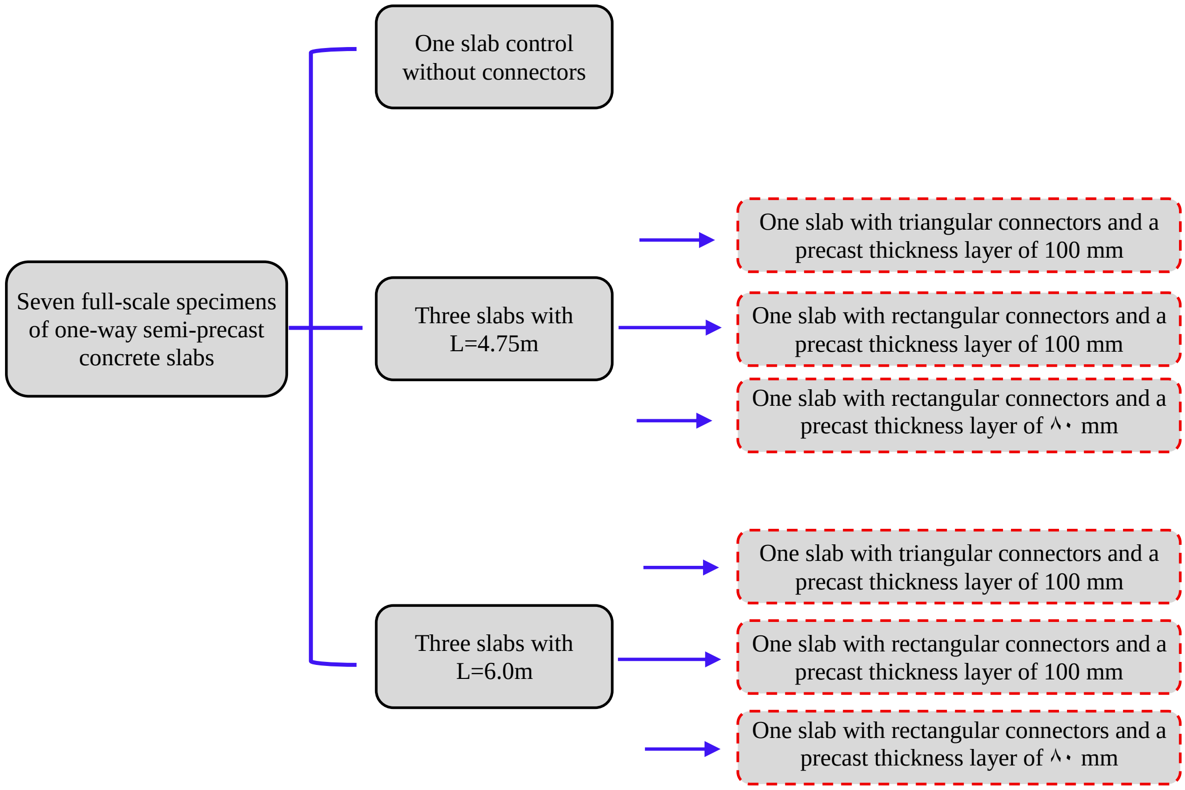

Figure 1. Methodological flowchart for the study on SPCSs' behavior

3. Experimental Program

3.1. Specimen Description

The experimental study involved seven full-scale specimens of one-way semi-precast concrete slabs. Each specimen had a cross-section of dimensions of 2000 mm × 200 mm. The total slab thickness consisted of a lower precast concrete section and a cast-in-place concrete topping layer (hereafter referred to as the "topping concrete layer"). These two components were designed to act together as a fully composite section. To ensure effective composite action and prevent slip at the interface, shear connectors were used as rigid connections. Various shapes and configurations of these connectors were employed to assess their effectiveness.

The slabs were designed in accordance with the provisions of the American Concrete Institute (ACI Committee 318, 2019) [29]. The pre-cast bottom layer was reinforced with 10 mm diameter reinforcing bars spaced at 150 mm intervals, while the cast-in-place top layer was reinforced with 8 mm diameter reinforcing bars spaced at 200 mm intervals.

The detailed dimensions of the specimens and the configuration of the reinforcing bars are presented in Table 1 and further illustrated schematically in Figures 2 and 3.

Table 1. Details of the test specimens

Slabs designation	Thickness of Precast Concrete Layer (mm)	Thickness of Cast-in-Place Concrete Layer	Size mm^3 Dimensions (l*b*t)	Shapes of Stirrups Used as Interface Connectors	Stirrups (Shear Connectors) Spacing (mm)
SPCS 1	100	100	6000×2000×200	Triangular	600
SPCS 2	100	100	6000×2000×200	Rectangular	600
SPCS 3	80	120	6000×2000×200	Rectangular	600
SPCS 4	100	100	4750×2000×200	Triangular	600
SPCS 5	100	100	4750×2000×200	Rectangular	600
SPCS 6	80	120	4750×2000×200	Rectangular	600
SPCS C	100	100	4750×2000×200	Without connection	600

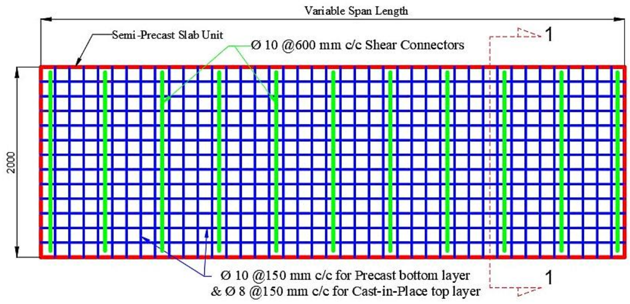

(a) Top view of the hybrid slab

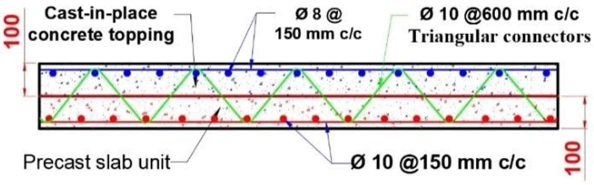

(b) Section (1-1) for specimens using triangular connectors

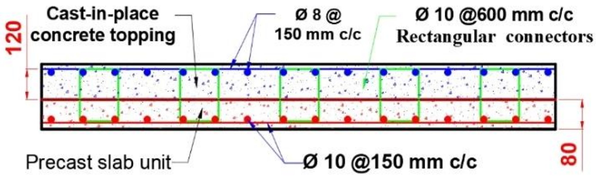

(c) Section (1-1) for specimens using rectangular connectors

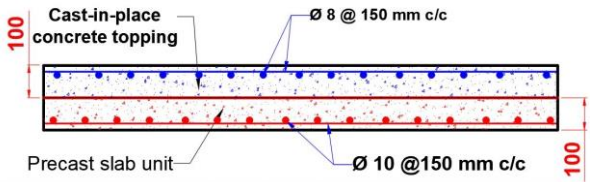

(d) Section (1-1) for the specimen without connectors

Figure 2. Reinforcement details and specimen dimensions

Reinforcement of pre-cast bottom layer

Reinforcement of cast-in-place topping layer

Reinforcement of rectangular and triangulate shear connectors

Figure 3. Detailed the production sequence of semi-precast concrete elements

3.2. Test Variables Specimen

The main variables investigated in the test specimens included:

- Connectors Shapes: Rectangular Connectors (RC) and Triangular Connectors (TC).
- Thicknesses of Precast Unit: 100 mm and 80 mm.
- Span Lengths: 4.75 meters and 6 meters.

For comparative analysis, a control specimen was prepared in the form of a two-layer concrete slab, consisting of a 100 mm-thick precast layer and a 100 mm-thick cast-in-place layer, constructed without the inclusion of shear connectors. This configuration was intended to evaluate the structural response of the composite system in the absence of mechanical interfacial reinforcement.

3.3. Casting Process

The casting process was carried out in two stages:

- Stage 1: The precast concrete portion of the slab was cast and properly cured for 28 days.
- Stage 2: After 28 days, once the precast unit had gained sufficient strength and approached the target compressive strength, cast-in-place topping concrete was poured over it. The topping concrete was then cured for an additional 28 days to ensure adequate bonding and strength development.

3.4. Material Properties

The concrete mixes were designed in accordance with the specifications outlined in ACI 211.1 [48]. In this study, a single mix design was used for both the precast and cast-in-place layers to achieve normal compressive strength. The mix consisted of 390 kg/m³ of cement, 1150 kg/m³ of coarse aggregate, and 760 kg/m³ of fine aggregate, with a water-to-cement ratio maintained at 0.42.

Following the completion of the mixing process, the workability of fresh concrete was assessed using the slump test, conducted in accordance with ASTM C143/C143M-20 [49]. To determine the compressive strength of the concrete mix, three cube specimens measuring 150 × 150 × 150 mm were cast and tested in accordance with BS EN 12390-3:2019 [50]. Each half-slab component (precast and cast-in-place) was constructed using the same normal concrete mix. For each half-slab, three cubic specimens were cast and cured under identical conditions during the production process. The average recorded compressive strength (f_{cu}) for both the precast and cast-in-place concrete was 35.8 MPa, and the measured slump value was 86 mm.

3.5. Materials Used in the Study

3.5.1. Cement

Ordinary Portland cement (Type I), locally manufactured in Basra, Iraq, was used in this study. The properties of this cement complied with the requirements of ASTM C150-19 [51]. Its chemical composition is presented in Table 2, while its physical properties are summarized in Table 3.

Table 2. Chemical properties of cement

	Chemical Components										Potential compounds			
Comp.	CaO	SiO_2	Al_2O_3	Fe_2O_3	MgO	SO3	L.O.I	Na_2O	K_2O	Insoluble residue	C3S	C2S	C3A	C4AF
Test result Contents (%)	63.11	20.5	5.11	4.1	2.46	2.26	2.19	0.29	0.62	0.51	51.9	17.8	2.52	13.2
Limits of ASTM C150-19 [51]	-	-	-	-	6.0 (max)	-	3.0 (max)	-	-	0.75 (max)	-	-	3.0 (max)	25.0 (max)

Table 3. Physical properties of cement

	Specific surface area (Blaine method) (m^2/kg)	Setting time (Vicat method) (min)		Compressive strength (MPa)		Specific gravity (g/cm^3)	Color
		Initial setting time	Final setting time	3 days	7 days		
Test result Contents (%)	310	140	295	17.2	23.8	3.15	Light grey
Limits of ASTM C150-19 [51]	Not less than 280	More than 45	Less than 375	More than 12	More than 19	---	---

3.5.2. Aggregates

The fine and coarse natural aggregates used in this study were obtained locally from the Safwan region in Basra Governorate**.** The fine aggregate exhibited a maximum particle size of 5 mm, while the coarse aggregate had a maximum size of 25 mm. Both aggregates were tested in accordance with the ASTM C33-23 [52] standard. The results confirmed that the gradation of both fine and coarse aggregates falls within the permissible limits defined by the specification. The physical properties of the fine and coarse aggregates are presented in Table 4, while their gradation curves are illustrated in Figure 4.

Table 4. Physical properties of coarse and fine aggregates

	Specific gravity	Sulfate content (SO_3) %	Water Absorption %	Bulk density (kg/m^3)	Maximum particle size (mm)
Coarse Aggregate	2.61	---	0.7	1518	19
Fine Aggregate	2.56	0.31	1.1	1678	5

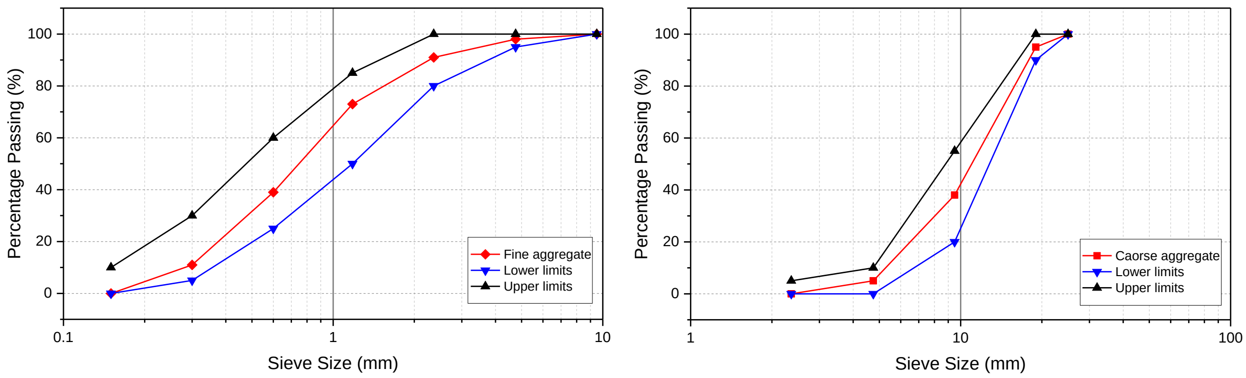

(a) (b)

Figure 4. Aggregate classification curves: (a) fine aggregate; (b) coarse aggregate

3.5.3. Steel Reinforcement

In this study, two sizes of conventional Grade 60 steel reinforcing bars were utilized: 10 mm and 8 mm nominal diameter. Their mechanical properties were experimentally evaluated. The 10 mm bars exhibited a yield strength of 417 MPa, an ultimate tensile strength of 573 MPa, and an elongation of 12.2%. Meanwhile, the 8 mm bars demonstrated a yield strength of 446 MPa, an ultimate tensile strength of 603 MPa, and an elongation of 11.8%. All measured properties conformed to the specifications outlined in ASTM A615-24 [53].

4. Experimental Program

4.1. Specimen Preparation and Curing

After twenty-eight days from casting the in-place concrete topping and upon completion of the curing process, the testing procedure was carried out. The semi-precast concrete slabs were placed on pre-prepared support structures.

4.2. Support Conditions

The pre-precast slabs were simply supported at both ends using pre-fabricated reinforced concrete beams, simulating simple support conditions. Each support beam had a width of 30 cm and was cast and prepared prior to the on-site casting of the slab. Special attention was given to ensuring proper alignment and secure position before the commencement of loading.

4.3. Loading Procedures

The load was applied using uniformly distributed cement bags, each weighing 50 kg, and was introduced gradually in stages with consistent increments of 250 kg per stage. At each loading stage, the load was held constant for 30 minutes prior to proceeding to the next increment, allowing sufficient time for deformation stabilization and crack development. Following each stabilization period, measurements of vertical deflection at the mid-span of the slab and separation at the external joints were recorded, as illustrated in Figure 5.

Figure 5. Loading arrangement for structural testing of semi-precast slabs

4.4. Instrumentation and Measurement

To monitor the vertical deflection of the slabs, a dial gauge with an accuracy of 0.02 mm was installed at the mid-span of each slab. Additionally, a horizontal dial gauge was mounted at the interface between the precast and cast-in-place concrete layers to measure the interface slip behavior. Figure 6 illustrates the layout and exact position of the dial gauges on the slab.

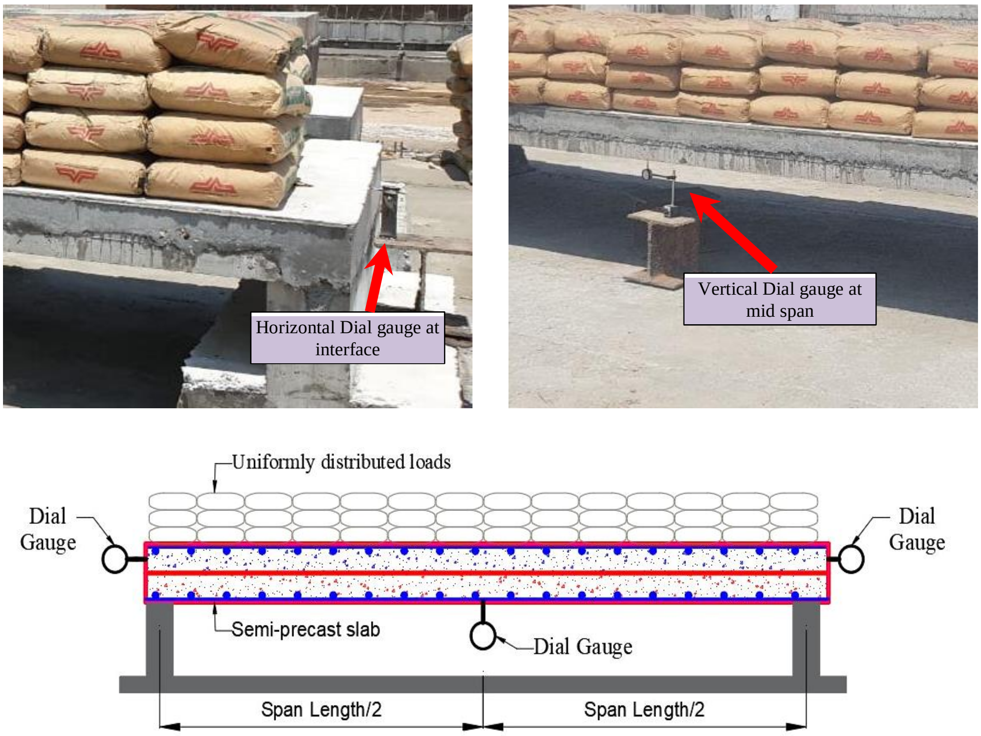

Figure 6. Illustrates the layout and exact positions of the dial gauges on the semi-precast slabs

5. Results and Discussion

5.1. Ultimate Load Capacity of Semi-Precast Slabs

Table 5 presents the experimental results for the semi-precast concrete slabs. The data indicate a significant improvement in the ultimate load capacity (Pu) of the slabs incorporating shear connectors, compared to the control specimen (SPCS C), which lacked such connectors and recorded the lowest ultimate load of 5.5 tons. Slabs reinforced with shear connectors exhibited considerable enhancements, with increases in ultimate load of 150.0%, 163.6%, and 186.4% for SPCS 4, SPCS 5, and SPCS 6, respectively, relative to the control slab (SPCS C). This improvement in load capacity performance is primarily attributed to the mechanical interlock developed at the interface between the precast and cast-in-place concrete layers, which enabled monolithic structural behavior. Among all specimens, SPCS 6-featuring rectangular shear connectors and a total thickness of 200 mm (80 mm precast and 120 mm cast-in-place), achieved the highest ultimate load of 15.75 tons. These findings highlight the essential role of shear connector design in enhancing the structural capacity of semi-precast concrete slab systems.

Table 5. Ultimate load capacity and mid-span deflection of tested slab specimens

Slab	First Cracking Load *Pcr* (tons)	Change in *Pcr* (%) $\frac{Pcri-Pcrc}{Pcrc}$	Ultimate Load *Pu* (tons)	Change in *Pu* (%) $\frac{Pui-Puc}{Puc}$%	Deflection at first Cracking (mm)	Deflection at ultimate load (mm)
SPCS 1	2	---	10.75	---	1.49	32.1
SPCS 2	2.25	---	11.25	---	1.4	30.8
SPCS 3	3	---	12.0	---	1.69	29.7
SPCS 4	2.5	100	13.75	150	1.41	24.5
SPCS 5	3.25	160	14.5	163.6	1.75	23.2
SPCS 6	4	220	15.75	186.4	1.76	21.8
SPCS C	1.25	---	5.5	---	1.45	14.4

The results clearly demonstrate that incorporating shear connectors at the interface substantially enhances both the loading capacity and flexural behavior of semi-precast slabs. The effectiveness of both rectangular connectors, as used in SPCS 2, SPCS 3, SPCS 5, and SPCS 6, and triangular connectors, as used in SPCS 1 and SPCS 4, confirms their potential application in structural systems that demand high performance and durability.

On the other hand, the influence of connector shape appears to be marginal. For instance, a slight increase of 4.65% in load capacity was recorded between SPCS 1 and SPCS 2, with utilized triangular and rectangular connectors, respectively. A similar trend was observed between SPCS 4 and SPCS 5, with a difference of only 5.45%, as shown in Table 5. This highlights the importance of selecting an appropriate shear connector, whether triangular or rectangular, to ensure the effectiveness of composite action.

Regarding slab thickness variations, a comparison between slabs with an 80 mm precast unit and a 120 mm cast-in-place layer showed only modest gains in ultimate load. SPCS 2 and SPCS 3 recorded a 6.67% increase, while SPCS 5 and SPCS 6 showed an 8.62% improvement. This result was also identified by Liu et al. [54]. Although the structural gains were limited, the reduction in precast slab thickness results in a lighter unit, facilitates transportation, increases the number of units transported per trip, and simplifies on-site handling. Finally, the effect of span length was found to be more significant. Reducing the span from 6.0 m to 4.75 m led to increases in ultimate load of 27.91%, 28.89%, and 31.25% for SPCS 1 versus SPCS 4, SPCS 2 versus SPCS 5, and SPCS 3 versus SPCS 6, respectively. These findings are consistent with those reported in a previous study [21]. These findings emphasize the combined influence of shear connector configuration, thickness, and span length on the performance of semi-precast concrete slabs. Furthermore, as shown in Table 5, the cracking load (Pcr) significantly increased in slabs SPCS 4, SPCS 5, and SPCS 6 by 100%, 160%, and 220%, respectively, when compared to SPCS C. This improvement is attributed to the enhancement of the concrete matrix due to the addition of shear connectors, which effectively delayed the initiation of cracking. In contrast, the control slab, which lacked connectors, exhibited a significantly lower cracking load, underscoring the importance of shear connectors in promoting composite action and structural cohesion. In addition, the use of rectangular shear connectors led to a significant increase in load-carrying capacity compared to triangular connectors, with improvements of 12.5% between SPCS 2 and SPCS 1, and 30.0% between SPCS 5 and SPCS 4. Furthermore, increasing the thickness of the cast-in-place concrete layer from 100 mm to 120 mm resulted in further improvements of 33.33% and 23.08% when comparing SPCS 3 to SPCS 2 and SPCS 6 to SPCS 5, respectively.

Three primary factors were identified as contributing to the increased load-carrying capacity of the hybrid (SPCS) concrete slabs. The first was the incorporation of shear connectors, which facilitated full composite action between the precast and cast-in-place concrete layers, enabling the slab to function as an integrated structural unit. The second factor involved the reduction of span length, which decreased flexural demands, thereby improving overall structural efficiency and allowing for more effective utilization of the composite section. The third was the increased thickness of the cast-in-place concrete layer, which enhanced flexural capacity by increasing the internal arm and the overall sectional strength. While the geometry of the shear connectors, such as rectangular or triangular shapes, plays a secondary role, the presence of shear connectors is essential to achieve structural integration and performance. Collectively, these factors result in improved strength, ductility, and crack strength, confirming the structural advantages of hybrid slab systems in both performance and constructability.

5.2. Load-Deflection Response

Figure 7 presents the load-deflection curves for the seven tested slab specimens. It can be observed that all specimens exhibited nearly identical behavior up to the initial cracking point, where the load-deflection relationship remained linear. The load-deflection response of the semi-precast slabs is generally characterized by a nonlinear pattern that can be divided into two distinct stages. The first stage is linear and elastic, corresponding to the uncracked state of the concrete, during which the contribution of the steel reinforcement is minimal. The second stage begins with the formation of the first visible crack, marking the transition to nonlinear behavior. At this point, tensile stresses are transferred from the cracked concrete to the reinforcement, leading to stress redistribution and the progressive development of multiple cracks. This outcome is consistent with the conclusions drawn by previous researchers [39, 41].

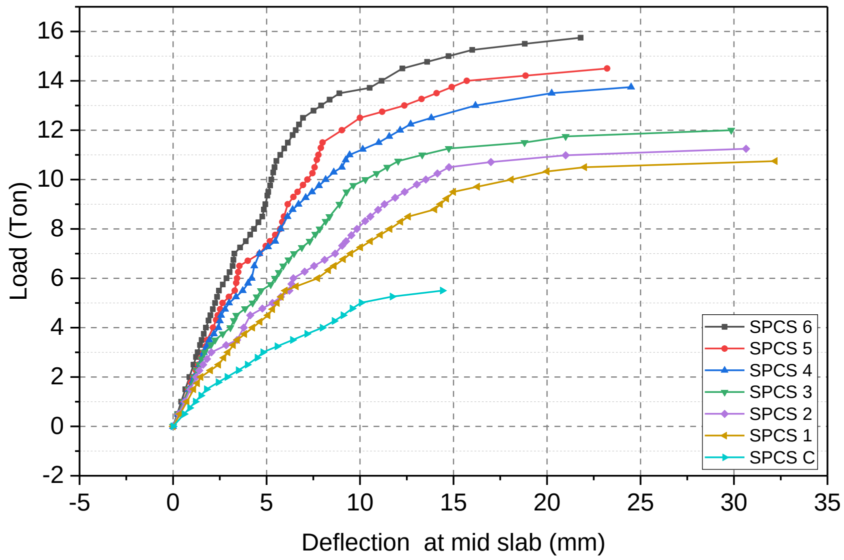

Figure 7. Load deflection curves of tested slabs

Notably, the mid-span deflection at ultimate load (Δu) increased significantly in specimens SPCS 1, SPCS 2, and SPCS 3 compared to the control slab (SPCS C). This increase indicates an improvement in the deformation capacity and a notable enhancement in the post-cracking stiffness of these specimens, thereby improving their ability to withstand additional loads and accommodate larger deformations. Consequently, reductions in the maximum deflection at ultimate load were recorded in SPCS 1, SPCS 2, and SPCS 3 by 70.1%, 61.1%, and 51.4%, respectively, compared to the control slab SPCS C. The effect of the connector geometry and changes in the thickness of the cast-in-place concrete layer on the deflection was relatively minor, with improvements of 4.05% and 5.31% observed between SPCS 1 and SPCS 2, and SPCS 4 and SPCS 5, respectively. Similarly, increasing the cast-in-place concrete thickness from 100 mm to 120 mm resulted in modest improvements of 3.57% between SPCS 2 and SPCS 3, and 6.03% between SPCS 5 and SPCS 6. Moreover, significantly lower deflection values were observed in these specimens at the same load level. This reduction in deflection is attributed to the increased post-cracking stiffness resulting from improved bonding and prevention of slip at the interface between the precast slab and the cast-in-place concrete. This enhancement was achieved through the presence of shear connectors, regardless of their geometry, which played a crucial role in enhancing both the stiffness and ductility of the composite slab system.

One of the primary factors contributing to the enhanced load-bearing capacity and deflection behavior of hybrid concrete slabs is the incorporation of shear connectors, which facilitate a combination of structural and material interactions that improve stiffness, ductility, and overall performance under flexural loads. The placement of shear connectors at the interface between the pre-cast and cast-in-place layers played a crucial role in significantly increasing post-cracking stiffness, thereby reducing deflection under equivalent load levels. Furthermore, these connectors effectively limited relative slip at the interface, promoting efficient stress transfer and allowing the slab to function as an integrated structural element. As a result, the slabs exhibited improved deformation capacity and smoother load transfer after the cracking stage. This more controlled and ductile response was further evidenced by the development of multiple, distributed cracks, rather than a localized failure. Additionally, the transition from elastic to the nonlinear cracked phase is managed more efficiently in specimens with connectors, which helps maintain load-bearing capacity even at advanced deformation stages. While variations in conductor geometry and cast-in-place thickness have minor effects on deflection values, their combined contribution still supports enhanced bonding conditions and interface integrity, resulting in an overall stiffer and more resilient flexible response.

5.3. Interface Slip

Figure 8 and Table 6 present the interface slip recorded between the precast concrete unit and the cast-in-place concrete layer at the ultimate load for all tested slab specimens. The results show a significant reduction in interface slip for specimens SPCS 4, SPCS 5, and SPCS 6, with improvements of 57.55%, 67.97%, and 69.27%, respectively, compared to the control specimen (SPCS C), which was constructed without shear connectors. These results are consistent with those previously documented by other researchers [30, 36, 41, 44]. This notable improvement is attributed to the enhanced mechanical interlock and bond strength at the interface provided by the inclusion of shear connectors, which facilitated more effective composite action.

Additionally, a comparison of connectors geometry showed that rectangular connectors were more effective at reducing interface slip compared to triangular connectors. Specifically, a 25.7% slip reduction was observed between SPCS 1 and SPCS 2, and a 24.5% reduction between SPCS 5 and SPCS 4, demonstrating that rectangular conductors are more effective than triangular conductors in improving separation. It was also observed that increasing the thickness of the cast-in-place concrete layer from 100 mm to 120 mm had minimal effect on reducing interface slip, indicating that thickness alone has a limited influence on interfacial bonding.

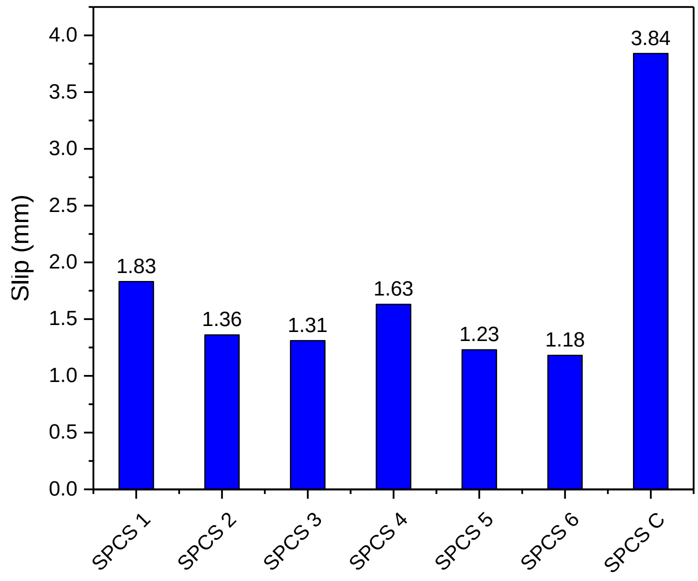

Figure 8. Interface slip responses of all tested specimens

Table 6. Interface slip and ductility index of the tested slab specimens

Slab designation	Interface slip (mm)	Change in slip (%)	Ultimate Deflection Δu (mm)	Yield deflection Δy (mm)	Ductility index $\mu = \frac{\Delta u}{\Delta y}$
SPCS 1	1.83	---	32.1	11.6	2.77
SPCS 2	1.36	---	30.8	10.4	2.96
SPCS 3	1.31	---	29.7	8.9	3.34
SPCS 4	1.63	-57.55*	24.5	8.6	2.85
SPCS 5	1.23	-68.49	23.2	7.7	3.01
SPCS 6	1.18	-69.27	21.8	6.4	3.41
SPCS C	3.84	---	14.4	8.3	1.73

Note: * Minus sign refers to the decreasing percentage.

As previously discussed, one of the primary factors contributing to the improved load-bearing capacity and enhanced load-deflection behavior of hybrid concrete slabs is the incorporation of shear connectors. These connectors play a crucial role in limiting the relative slip between the precast and cast-in-situ concrete layers, thereby prompting the composite action. The geometry of the shear connectors significantly impacted slip performance, with rectangular connectors demonstrating superior effectiveness compared to triangular ones. This is attributed to their larger contact surface area and stronger mechanical bonding with the surrounding concrete. Conversely, increasing the thickness of the cast-in-place concrete layer exhibited only a minor effect on mitigating interface slip. Thus, the reduction in interface slip is primarily governed by improved bonding, optimized stress distribution, and effective shear transfer at the interface—factors that are essential for achieving reliable and efficient performance in composite slab systems.

5.4. Ductility Behavior of Semi-precast Concrete Slabs

Ductility refers to a structural element's ability to undergo significant inelastic deformation and dissipate energy after reaching its elastic limit, without experiencing abrupt failure. It is typically quantified as the ratio of the deflection at the ultimate load (Δu) to the deflection at the yield point (Δy) or the onset of cracking. In semi-precast concrete slabs, ductility serves as a critical measure of structural robustness, particularly in evaluating the composite action between the precast concrete unit and the cast-in-place (CIP) concrete topping. A higher ductility ratio reflects improved post-cracking performance and greater deformation capacity, both of which are essential for ensuring safety and structural integrity. In this study, the yield deflection (Δy) was defined as the mid-span deflection corresponding to 75% of the ultimate load, following established methodologies in the literature [55–58]. The experimental results, as presented in Figure 9 and Table 6, reveal substantial improvement in the ductility for slabs incorporating shear connectors when compared to the control specimen (SPCS C), which did not include these connectors. Specifically, ductility ratios increased by 64.74%, 73.99%, and 97.11% for SPCS 4, SPCS 5, and SPCS 6, respectively, compared to the control specimen (SPCS C). Similar results have been reported in previous studies [35, 39]. Furthermore, rectangular shear connectors outperformed triangular ones, yielding ductility improvements of 6.86% and 5.61% between SPCS 1 and SPCS 2, and SPCS 4 and SPCS 5, respectively. Increasing the thickness of the cast-in-place concrete from 100 mm to 120 mm also led to ductility enhancement of 12.84% (SPCS 2 vs. SPCS 3) and 13.29% (SPCS 5 vs. SPCS 6). These results highlight the important role that shear connector design and cast-in-place layer thickness play improving the ductility and overall structural performance of SPCS systems.

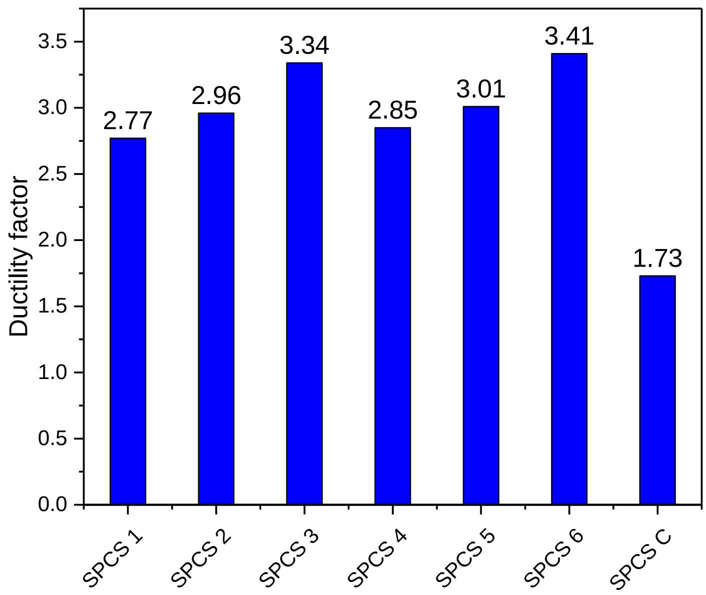

Figure 9. Ductility factor of all tested specimens

One of the main factors contributing to the observed enhanced in the ductility behavior of the hybrid concrete slabs is the incorporation of shear connectors. These connectors facilitate efficient stress transfer and ensure continuity across the interface, thereby enabling the slab to accommodate additional deformations beyond the cracking stage without experiencing sudden failure. The reduced in interface slip contributed to a more uniform stress distribution, resulting in a smoother post-cracking response and increased energy dissipation. The geometry of the shear connectors significantly impacted ductility performance, with rectangular connectors demonstrating superior effectiveness compared to triangular ones, owing to their larger surface area and improved mechanical interlock. Furthermore, the increased thickness of the cast-in-place concrete layer significantly contributed to the improved ductility. These factors led to significantly improved the deformation capacity and overall ductility of the hybrid slab system.

5.5. Structural Stiffness and Energy Absorption Properties

Initial stiffness refers to the slope of the load-deflection curve during the uncracked elastic phase of a structural element. In this study, initial stiffness was calculated following the methodology outlined in references [59–62]. For semi-precast concrete slabs, a higher initial stiffness indicates increased strength to deformation under service loads, thereby enhancing overall serviceability and minimizing deflections prior to the onset of cracking.

Table 7 displays the initial stiffness values for the tested specimens. Substantial improvements in initial stiffness were observed in specimens SPCS 4, SPCS 5, and SPCS 6, which exhibited increases of 105.81%, 116.28%, and 163.95%, respectively, compared to the control specimen (SPCS C). The influence of shear connector type, comparing rectangular and triangular shapes, was relatively minor. It resulted in a 20.15% increase in stiffness between SPCS 1 and SPCS 2, and only 5.08% between SPCS 4 and SPCS 5. Conversely, increasing the thickness of the cast-in-place concrete layer led to more noticeable improvements in initial stiffness: 10.56% between SPCS 2 and SPCS 3, and 22.04% between SPCS 5 and SPCS 6. These findings affirm that in semi-precast concrete slabs, higher initial stiffness contributes to greater strength against early-stage deformation under service loads, thereby enhancing serviceability and effectively limiting deflections prior to the onset of cracking.

Table 7. Experimental results: stiffness and energy absorption of the slabs

Slab designation	Pcr Crack (tons)	Deflection at first crack (mm)	Initial stiffness (tons /mm)	Change in Initial stiffness (%)	Energy Dissipation Capacity (tons.mm)	Change in Energy Dissipation Capacity (%)
SPCS 1	2	1.49	1.34	---	262.21	---
SPCS 2	2.25	1.4	1.61	---	267.6	---
SPCS 3	3	1.69	1.78	---	282.23	---
SPCS 4	2.5	1.41	1.77	105.81	253.6	388.07
SPCS 5	3.25	1.75	1.8.6	116.28	258.96	398.38
SPCS 6	4	1.76	2.27	163.95	265.7	411.35
SPCS C	1.25	1.45	0.86	---	51.96	---

On the other hand, energy dissipation capacity is a critical parameter that reflects a structural slab's ability to absorb and dissipate energy, particularly under cyclic or dynamic loading conditions. In this study, energy dissipation was evaluated based on the methodology described in previous studies [62, 63].

This attribute is of parameter importance in seismic applications, where structures are subjected to repeated stress reversals. In semi-precast concrete slabs, improved energy dissipation, primarily achieved through the incorporation of shear connectors and improved interfacial bonding, contributes significantly to structural resilience by delaying the onset of failure and reducing cumulative damage. These energy dissipation mechanisms complement other structural properties, such as initial stiffness and ductility, ensuring that the slabs maintain performance under both service and extreme load conditions.

Experimental results, as shown in Table 7, demonstrate significant improvements in energy dissipation for specimens SPCS 4, SPCS 5, and SPCS 6, with increases of 388.07%, 398.38%, and 411.35%, respectively, compared to the control slab (SPCS C), which lacked shear connectors. These improvements underscore the dominant role of shear connectors in facilitating effective composite action. Conversely, the effect of connector geometry was relatively modest, with rectangular connectors resulting in only marginal gains, with a 2.06% increase between SPCS 1 and SPCS 2, and 2.11% between SPCS 4 and SPCS 5. Similarly, increasing the thickness of the cast-in-place concrete layer from 100 mm to 120 mm produced slight improvements in energy dissipation: 5.47% for SPCS 2 versus SPCS 3, and 2.6% for SPCS 5 versus SPCS 6. The findings suggested that although variations in connector geometry and cast-in-place concrete thickness may contribute marginally, the predominant factor governing energy dissipation is the effectiveness of the shear transfer mechanism. Therefore, optimizing shear connectivity emerges as the principal strategy for improving energy dissipation capacity and enhancing the overall seismic performance of semi-precast slab systems.

The observed enhancements in both initial stiffness and energy dissipation of the semi-precast concrete slabs are primarily attributed to the incorporation of shear connectors, which significantly improve structural continuity and interfacial bonding between the precast and cast-in-place concrete layers. These connectors effectively mitigate interface slip and facilitate efficient shear transfer, thereby increasing strength to early-stage deformations and enhancing pre-cracking stiffness. Although the influence of connector geometry was relatively modest, rectangular connectors demonstrated slightly superior performance, attributed to their mechanical interlocking and greater contact service with the surrounding concrete. Moreover, increasing the thickness of the cast-in-place concrete contributed to improved section depth and flexural rigidity, further enhancing stiffness.

Regarding energy dissipation, shear connectors significantly increase the slab's ability to absorb and release energy under cyclic or dynamic loading, delaying failure and reducing damage accumulation. This improvement is particularly important in seismic applications, where ductile behavior and repeated energy absorption are vital. Although connector shape and concrete thickness had minor effects, the dominant factor influencing both stiffness and energy dissipation was the existence of a well-detailed shear connection system that enabled efficient composite action.

5.6. Failure Modes

The experimental study investigation revealed that the failure modes across all tested semi-precast slab specimens were generally consistent, with flexural failure being the predominant mode. This result is consistent with previous researchers [21, 30, 39, 41]. This flexural behavior was characterized by the formation and propagation of multiple cracks along the span, particularly near the mid-span region, followed by reinforcement yielding and increased crack development, as shown in Figure 10-a. Notably, the only exception was the control specimen (SPCS C), which failed through interface debonding between the precast concrete unit and the cast-in-place layer due to the absence of shear connectors, as shown in Figure 10-b. This type of failure occurred prematurely and limited the specimen's load-carrying capacity, emphasizing the critical role of mechanical interlock in achieving effective composite behavior.

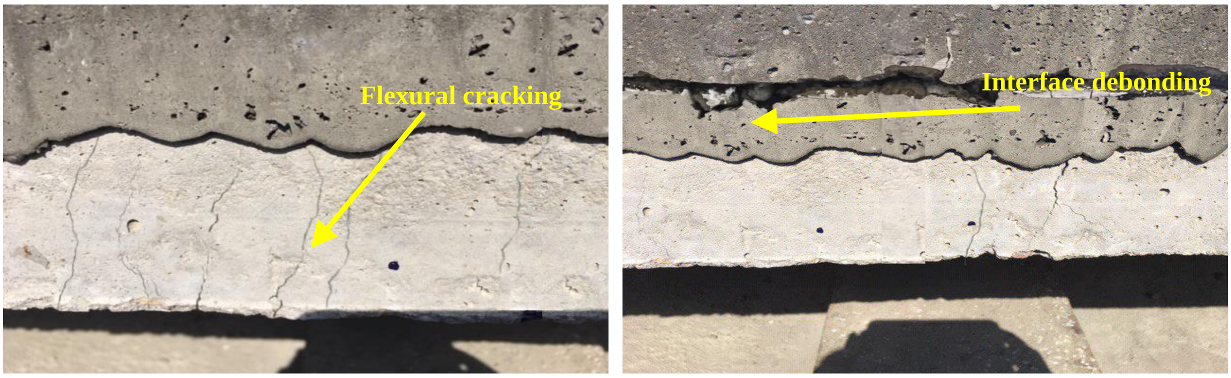

(a) (b)

Figure 10. Typical failure mode of semi-precast slabs

As shown in Figure 10-a, specimens equipped with shear connects demonstrated enhanced structural integrity, effectively delaying the onset of cracking and distributing stress more uniformly across the interface. These connectors not only contributed to a significant increase in ultimate load capacity but also improved the post-cracking stiffness of the slabs, allowing for additional deformation capacity before failure. The enhanced ductility enabled the slabs to sustain more extensive crack development without compromising overall structural performance. Furthermore, while different connector geometries, such as triangular and rectangular, and variations in the thickness of the cast-in-place concrete layer were evaluated, their influence on the overall failure mode was minimal.

The incorporation of shear connectors played a pivotal role in improving the failure behavior of the hybrid concrete slabs by enhancing the bond between the precast and cast-in-place concrete layers. These connectors facilitate mechanical interlocking at the interface, thereby preventing delamination and enabling the slab to behave as a unified structural system. Consequently, early separation—which typically occurs in the absence of shear connectors, as observed in the control specimen—was avoided, and the failure mode shifted to a more favorable ductile flexural failure. This transition was characterized by progressive crack propagation, reinforcing yielding, and enhanced structural performance beyond the cracking stage. Although variations in connector geometry and cast-in-place layer thickness had some influence on stiffness and ductility, they did not significantly alter the overall failure mechanism. Therefore, the primary reason for the improved failure pattern lies in the reliable shear transfer across the interface, which preserves structural continuity and allows the slab to reach its full flexural capacity before failure.

6. Theoretical Load Capacity and Comparison with Experimental Results

In the design of single-reinforced concrete sections, the nominal flexural strength (Mn) is a critical parameter determined based on the internal forces balance and strain compatibility. American Concrete Institute (ACI Committee 318, 2019) [29], particularly Section 22.2.2, provides the basis for calculating flexural strength using the rectangular stress block approach.

The nominal moment capacity (Mn) is given by the following equation:

$$Mn = As * f_y(d - \frac{a}{2}) \tag{1}$$

whereas is area of tensile reinforcement (mm²), f_y is yield strength of steel reinforcement (MPa), d is effective depth of section (mm), and a is depth of equivalent rectangular stress block (mm), calculated by the following equation:

$$a = \frac{As * f_y}{0.85 * f_c' * b} \tag{2}$$

f_c' is compressive strength of concrete (MPa), and b is width of section (mm).

Assuming full composite action and uniform material properties across all specimens, the calculated nominal flexural moment capacity was determined to be 74.41 kN.m. This value reflects the ideal behavior of a composite section where no slip occurs at the interface between the precast and cast-in-place concrete layers. In this context, the flexural capacity was also used to represent the behavior of a homogeneously cast slab, which is generally considered to exhibit superior structural performance due to its continuous material interface and fully bonded cross-section.

Although a monolithic slab was cast nor tested in this study, its theoretical performance was approximated by assuming ideal composite action within semi-precast slab systems. This approach was considered appropriate for comparison purposes, as the mechanical behavior of a monolithic slabs under flexural loads is well documented in the available literature. Furthermore, the decision to omit a monolithically cast specimen was driven by economic considerations. This allowed the experimental program to focus on evaluating the performance of semi-precast configurations incorporating various types and geometries of shear connectors.

Accordingly, the theoretical flexural capacity—calculated based on the assumption of full composite behavior—was used as a control for an equivalent a monolithic slab. This theoretical assumption provided a benchmark for assessing the effectiveness of shear connectors and the degree of composite interaction achieved in the tested hybrid slab specimens. The theoretical evaluation of the flexural strength capacity of semi-precast concrete slabs (SPCS) was performed using classical elastic beam theory for simply supported members subjected to uniform distributed loads, in accordance with ACI 318-19 [29]. Since all tested slabs were simply supported along their shorter edges and subjected to full-span loading, the maximum mid-span bending moment was determined using the standard elastic bending equation for uniform distributed loads:

$$Mn = \frac{Wn * l^2}{8} \quad \Rightarrow \quad Wn = \frac{Mn * 8}{l^2} \tag{3}$$

where *Wn* is the corresponding uniformly distributed load, and l is the span length.

In this study, only the compressive strength of the cubes was measured. To obtain the equivalent cylinder compressive strength, a conversion relationship reported in the literature [64, 65] was used, ensuring consistency with previously applied formulas. This relationship is expressed in the following equation:

$$f_{cylider} = 0.8 * f_{cube} \tag{4}$$

Two slab configurations were analyzed: the first with a total thickness of 200 mm, a width of 2000 mm, and a span of 6000 mm; and the second with the same cross-sectional dimensions and a shorter span of 4750 mm. A nominal moment capacity of 74.41 kN.m was adopted in both cases. Based on this value, the corresponding distributed loads were calculated as 16.53 kN/m for the 6.0 m span and 26.38 kN/m for the 4.75 m span.

To enable direct comparison with the experimental results—which were recorded in terms of the total applied load—these distributed loads were converted to total loads by multiplying by the respective slab spans. The resulting theoretical nominal load capacities were 99.21 kN for the longer-span slab and 125.32 kN for the shorter one. These values served as reference points for assessing the structural efficiency and composite behavior of the tested slabs. For consistency in comparison, the theoretical values were converted from kilonewtons to tons, as shown in Table 8.

Table 8. Theoretical and experimental nominal load of slabs

Slabs designation	Size Dimensions (l*b*t) - mm³	Theoretical Nominal Loads (tons)	Experimental Nominal Loads (tons)	Change (%)
SPCS 1	6000×2000×200	9.92	10.75	8.36
SPCS 2	6000×2000×200		11.25	13.4
SPCS 3	6000×2000×200		12.0	20.96
SPCS 4	4750×2000×200	12.53	13.75	9.72
SPCS 5	4750×2000×200		14.5	15.7
SPCS 6	4750×2000×200		15.75	25.68
SPCS C	4750×2000×200		5.5	-56.11

The experimental outcomes presented in Table 8 and Figure 11 demonstrate a consistent and significant enhancement in the load-carrying capacity of the semi-precast concrete slabs (SPCSs) compared to theoretical predictions based on ACI 318-19 [29]. This improvement is primarily attributed to the inclusion of shear connectors, which played a pivotal role in establishing effective composite action between the precast and cast-in-place (CIP) concrete layers. For the specimens with a 6-meter span (SPCS 1, SPCS 2, and SPCS 3), the experimental ultimate loads exceeded theoretical values by 8.36%, 13.4%, and 20.96%, respectively, as illustrated in Figure 11-a. These results highlight the importance of well-designed shear connectors in fully mobilizing the composite cross-section, reducing interface slip, and enabling the slab system to act as a unified structural element. The performance gains were even more pronounced in the shorter-span specimens (SPCS 4, SPCS 5, and SPCS 6), where the reduced span length of 4.75 meters led to notably higher structural efficiency.

As shown in Figure 11-a, these slabs exceeded theoretical predictions by 9.72%, 15.7%, and 25.68%, respectively. This trend reflects the inherent reduction in flexural demands associated with shorter spans, which in turn lowers interfacial shear stresses and facilitates more effective stress transfer across the precast and cast-in-place concrete interface. The inclusion of shear connectors—particularly when combined with the more favorable moment distribution in the shorter spans—enhances strain compatibility and promotes improved energy dissipation. This interaction ultimately contributes to the increased load-carrying capacity and superior overall performance of the composite slab system. A particularly noteworthy observation was the performance of the control specimen (SPCS C), which was constructed without any shear connectors. This specimen exhibited a 56.11% reduction in ultimate load capacity compared to the theoretical prediction- an outcome that not only indicates a loss in strength but also reflects a complete shift in the failure mechanism. The absence of the composite action caused the precast and cast-in-place (CIP) concrete layers to act independently, resulting in premature debonding and a flexural shear failure localized at the interface. This finding underscores the critical importance of effective mechanical shear transfer in achieving the intended structural integrity and load-bearing performance of composite slab systems.

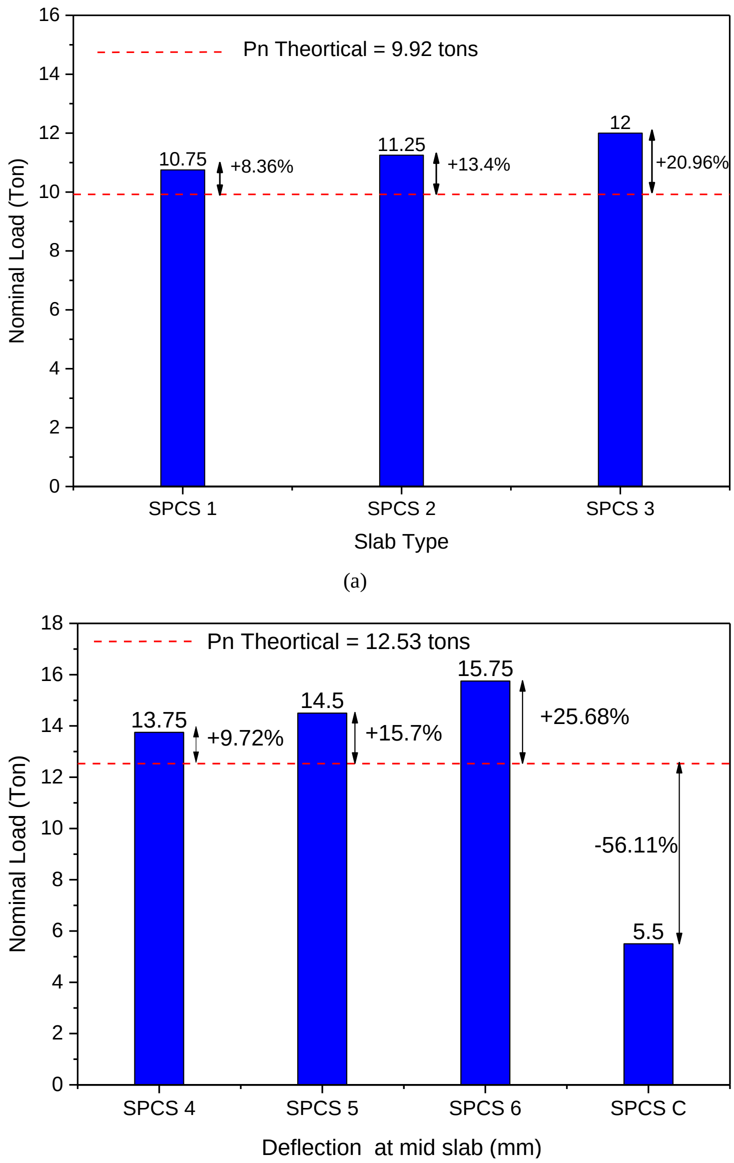

(a)

(b)

Figure 11. Comparison between the theoretical and experimental load capacity

These findings collectively confirm the conservative nature of ACI 318-19 [29] in predicting the flexural performance of hybrid slab systems. While this code offers a reliable and safe design baseline, the experimental results demonstrate that actual load-carrying capacities can significantly exceed theoretical values when shear connectors are properly designed and implemented. This highlights the crucial role of refined interface details in realizing the full structural potential of composite systems. Moreover, the outcomes suggest that existing code provisions could be further enhanced or supplemented with composite efficiency factors to more accurately represent the performance of well-detailed semi-precast slabs. Although the observed improvements in ultimate capacity ranged from approximately 7% to 25%, these gains are structurally meaningful, particularly in the broader context of construction efficiency and design optimization. Even modest enhancements in structural capacity can yield considerable benefits in load distribution, serviceability, and material utilization. Beyond strength improvements, semi-prefabricated composite systems offer several inherent advantages that make them highly viable for modern construction practices. These include accelerated construction timelines due to reduced on-site formwork and curing requirements, improved quality control through factory-based fabrication, and decreased labor demands and construction costs-especially in large-scale or repetitive projects. Additionally, the utilization of lightweight precast components facilitates transportation and on-site handling while maintaining structural efficiency. Enhanced composite action, achieved through effective shear transfer mechanisms, ensures efficient load distribution and improved crack control. Furthermore, the system offers consideration design flexibility, enabling accommodation of varying span lengths, section depths, and architectural specifications.

Therefore, when the system-level advantages are considered in conjunction with the observed enhancements in structural performance, even modest increases in load-carrying capacity become highly significant. The semi-precast construction approach promotes efficient utilization of material and optimal resource allocation, while also delivering durable and structurally robust slab systems. The findings of this study not only affirm the conservative nature of ACI 318-19 [29] as a dependable design guideline but also illustrate that, with appropriate interface detailing, actual slab performance can exceed code-based predictions. Collectively, these advantages highlight the strong potential of semi-precast concrete systems for applications where construction efficiency, quality assurance, and structural reliability are of critical importance.

7. Conclusion

This experimental study evaluated the structural performance of semi-precast concrete slabs (SPCSs) incorporating various shear connector configurations, cast-in-place (CIP) concrete thicknesses, and span lengths. The findings revealed that integrating shear connectors into SPCSs markedly enhanced their behavior across multiple structural parameters in comparison to the non-composite control specimen (SPCS C). Rectangular connectors, in particular, established a strong mechanical interlock at the interface between precast and CIP layers, promoting effective composite action and structural continuity. This resulted in substantial improvements in the ultimate load capacity, which increased by 150.0%, 163.6%, and 186.4% for SPCS 4, SPCS 5, and SPCS 6, respectively. Cracking loads similarly increased by 100%, 160%, and 220% in these specimens. The presence of shear connectors also contributed to improved serviceability, as demonstrated by notable reductions in mid-span deflection at ultimate load, ranging from 51.4 to 70.1% for SPCS 1 through SPCS 3.

Additionally, interface slip was significantly reduced in the connector-reinforced slabs, and ductility ratios showed substantial gains, indicating improved deformation capacity and post-cracking behavior. Initial stiffness was notably enhanced, particularly in SPCS 6, which recorded a 163.95% increase compared to the control slab. Energy dissipation capacity also improved dramatically, reaching a maximum increase of 411.35%. While the presence of shear connectors was the dominant factor in performance enhancement, rectangular connectors generally produced better results than triangular ones, particularly in minimizing interface slip and improving ductility. Variation in CIP thickness and span length had measurable but secondary effects on overall behavior. Importantly, all specimens with connectors exhibited ductile flexural failure, in contrast to the brittle interface debonding observed in the control slab. These results confirm that well-detailed shear connectors are essential for achieving monolithic behavior in hybrid slab systems. Furthermore, the close agreement between the experimental outcomes and theoretical predictions based on ACI 318-19 and elastic beam theory validated the applicability of such models for designing efficient and reliable semi-precast slab structures in modern construction practices.

It is suggested that future studies explore the long-term behavior, fatigue performance, and cyclic loading response of various connector configurations. Additionally, full-scale testing under real-world conditions would further validate these findings and contribute to the development of standardized design codes for semi-precast slabs.

8. Declarations

8.1. Author Contributions

Conceptualization, K.Z. and H.A.; methodology, H.A.; software, K.Z.; validation, M.D., A.A., and K.Z.; formal analysis, H.A.; investigation, M.S.; resources, M.D.; data curation, M.S.; writing—original draft preparation, A.A.; writing—review and editing, A.A.; visualization, A.Z.; supervision, A.Z. and K.Z. All authors have read and agreed to the published version of the manuscript.

8.2. Data Availability Statement

The data presented in this study are available on request from the corresponding author.

8.3. Funding

The authors received no financial support for the research, authorship, and/or publication of this article.

8.4. Conflicts of Interest

The authors declare no conflict of interest.

9. References

[1] Mohamed, M. S., Thamboo, J. A., & Jeyakaran, T. (2020). Experimental and numerical assessment of the flexural behaviour of semi-precast-reinforced concrete slabs. Advances in Structural Engineering, 23(9), 1865-1879. doi:10.1177/1369433220904011.

[2] Xiong, F., Zou, H., & Lu, Y. (2023). A macro element of demountable bolted steel-concrete composite connections for a novel prefabricated concrete sandwich wall panel structure. Engineering Structures, 293, 116571. doi:10.1016/j.engstruct.2023.116571.

[3] Pu, W., Zhang, Q., Jia, Q., Wei, W., & Li, B. (2024). Full-scale load testing for evaluating crack performance in precast prestressed concrete communication towers with annular sections. Results in Engineering, 24, 103395. doi:10.1016/j.rineng.2024.103395.

[4] Ristic, J., Misini, L., Ristic, D., & Hristovski, V. (2024). Upgrading of Precast Roof Beam–Column Connections with Seismic Safety Key Devices. Civil Engineering Journal (Iran), 10(5), 1437–1454. doi:10.28991/CEJ-2024-010-05-06.

[5] Nodehi, M., & Mohamad Taghvaee, V. (2022). Sustainable concrete for circular economy: a review on use of waste glass. Glass Structures & Engineering, 7(1), 3-22. doi:10.1007/s40940-021-00155-9.

[6] Chen, G. Q., Wu, H., Cheng, Y. H., & Lu, J. X. (2025). Comparative studies on blast resistance of precast concrete composite and cast-in-place slabs. Journal of Building Engineering, 113077. doi:10.1016/j.jobe.2025.113077.

[7] Al-Fasih, M. Y. M., Edris, W. F., Elbialy, S., Marsono, A. K., & Al Sayed, A. A. K. A. (2024). Lateral Displacement Behavior of IBS Precast Concrete Elements Reinforced with Dual System. Civil Engineering Journal (Iran), 10(1), 317–335. doi:10.28991/CEJ-2024-010-01-020.

[8] Hidayawanti, R., Latief, Y., & Gaspersz, V. (2024). Risk-Based Method-Technology Integration on Spun Pile Production for Product and Service Quality. Civil Engineering Journal (Iran), 10(11), 3683–3698. doi:10.28991/CEJ-2024-010-11-015.

[9] Afefy, H. M., Heniegal, A. M., Baraghith, A. T., Ibrahim, O. M. O., & Eldwiny, M. E. A. (2024). Flexural Behavior of RC Continuous Beams Strengthened by Cementitious Composite Materials. Civil Engineering Journal (Iran), 10(9), 2839–2858. doi:10.28991/CEJ-2024-010-09-05.

[10] Fan, C., Binchao, D., & Yin, Y. (2023). Hierarchical structure and transfer mechanism to assess the scheduling-related risk in construction of prefabricated buildings: An integrated ISM–MICMAC approach. Engineering, Construction and Architectural Management, 30(7), 2991-3013. doi:10.1108/ECAM-09-2021-0785.

[11] Putra, W. T., Setiawan, A. F., Saputra, A., Satyarno, I., & Pratama, H. Y. (2024). Frictional Axial Resistance of Clamped Split Pocket Mechanism Steel Structural Joint: An Experimental Study. Civil Engineering Journal (Iran), 10(9), 2870–2887. doi:10.28991/CEJ-2024-010-09-07.

[12] Tam, V. W. Y., Fung, I. W. H., Sing, M. C. P., & Ogunlana, S. O. (2015). Best practice of prefabrication implementation in the Hong Kong public and private sectors. Journal of Cleaner Production, 109, 216–231. doi:10.1016/j.jclepro.2014.09.045.

[13] Kadir, M. R. A., Lee, W. P., Jaafar, M. S., Sapuan, S. M., & Ali, A. A. A. (2006). Construction performance comparison between conventional and industrialised building systems in Malaysia. Structural Survey, 24(5), 412-424. doi:10.1108/02630800610712004.

[14] Akmam Syed Zakaria, S., Gajendran, T., Rose, T., & Brewer, G. (2018). Contextual, structural and behavioural factors influencing the adoption of industrialized building systems: a review. Architectural Engineering and Design Management, 14(1–2), 3–26. doi:10.1080/17452007.2017.1291410.

[15] Shen, L. Y., Tam, V. W. Y., & Li, C. Y. (2009). Benefit analysis on replacing in situ concreting with precast slabs for temporary construction works in pursuing sustainable construction practice. Resources, Conservation and Recycling, 53(3), 145-148. doi:10.1016/j.resconrec.2008.11.001.

[16] Lee, J. D., Yoon, J. K., & Kang, T. H.-K. (2016). Combined half precast concrete slab and post-tensioned slab topping system for basement parking structures. Journal of Structural Integrity and Maintenance, 1(1), 1–9. doi:10.1080/24705314.2016.1153281.

[17] Cho, K., Shin, Y., & Kim, T. (2017). Effects of Half-Precast Concrete Slab System on Construction Productivity. Sustainability, 9(7), 1268. doi:10.3390/su9071268.

[18] Youn, S.-G., & Cho, G.-D. (2011). Experimental Study on the Cracking Loads of LB-DECKs with Varied Cross-Section Details. Journal of the Korea Concrete Institute, 23(5), 657–665. doi:10.4334/jkci.2011.23.5.657.

[19] Figueiredo Filho, J. R., & Shiramizu, A. K. H. (2011). Design, production, and execution of buildings with precast lattice slabs. IBRACON Journal of Structures and Materials, 4(1), 123–146. doi:10.1590/s1983-41952011000100007. (In Portuguese).

[20] Löfgren, I. (2003). Lattice Girder Elements-Investigation of Structural Behaviour and Performance Enhancements. Nordic Concret Research, 1, 85-104.

[21] Qi, J., & Yang, H. C. (2021). Improvement of a truss-reinforced, half-concrete slab floor system for construction sustainability. Sustainability (Switzerland), 13(7), 3731. doi:10.3390/su13073731.

[22] Mahmutović, P. A., & Žuna, Š. (2011). Trends in the improvement of lattice girders production technology in steelwork zenica. 15th International Research/Expert Conference, Trends in the Development of Machinery and Associated Technology (TMT 2011), 12-18 September, 2011, Prague, Czech.

[23] Newell, S., & Goggins, J. (2019). Experimental study of hybrid precast concrete lattice girder floor at construction stage. Structures, 20, 866–885. doi:10.1016/j.istruc.2019.06.022.

[24] Momayez, A., Ehsani, M. R., Ramezanianpour, A. A., & Rajaie, H. (2005). Comparison of methods for evaluating bond strength between concrete substrate and repair materials. Cement and Concrete Research, 35(4), 748–757. doi:10.1016/j.cemconres.2004.05.027.

[25] Júlio, E. N. B. S., Branco, F. A. B., & Silva, V. D. (2004). Concrete-to-concrete bond strength. Influence of the roughness of the substrate surface. Construction and Building Materials, 18(9), 675–681. doi:10.1016/j.conbuildmat.2004.04.023.

[26] Ashteyat, A. M., Al Rjoub, Y. S., Obaidat, A. T., & Dagamseh, H. (2019). Strengthening and repair of one-way and two-way self-compacted concrete slabs using near-surface-mounted carbon-fiber-reinforced polymers. Advances in Structural Engineering, 22(11), 2435–2448. doi:10.1177/1369433219843649.

[27] Asad, M., Dhanasekar, M., Zahra, T., & Thambiratnam, D. (2019). Characterisation of polymer cement mortar composites containing carbon fibre or auxetic fabric overlays and inserts under flexure. Construction and Building Materials, 224, 863–879. doi:10.1016/j.conbuildmat.2019.07.120.

[28] Thamboo, J. A., & Dhanasekar, M. (2015). Characterisation of thin layer polymer cement mortared concrete masonry bond. Construction and Building Materials, 82, 71–80. doi:10.1016/j.conbuildmat.2014.12.098.

[29] ACI 318-19. (2019). Building Code Requirements for Structural Concrete and Commentary. American Concrete Institute (ACI), Farmington Hills, United States. doi:10.14359/51716937.

[30] Mohamed, M. S., Thamboo, J. A., & Jeyakaran, T. (2020). Experimental and numerical assessment of the flexural behaviour of semi-precast-reinforced concrete slabs. Advances in Structural Engineering, 23(9), 1865–1879. doi:10.1177/1369433220904011.

[31] Hillebrand, M., Sinning, A., & Hegger, J. (2024). Shear and interface shear fatigue of semi-precast slabs with lattice girders under cyclic loading. Structural Concrete, 25(6), 4895–4917. doi:10.1002/suco.202400219.

[32] Zając, J., Drobiec, Ł., Jasiński, R., Mazur, W., Grzyb, K., & Kisiołek, A. (2020). Research on semi-precast prestressed concrete slab under short-term and long-term load. MATEC Web of Conferences, 323, 02001. doi:10.1051/matecconf/202032302001.

[33] Lee, Y. L., Karim, a. T. a, Ismail, a R., Chai, T. J., Koh, H. B., Nagapan, S., & Yeoh, D. (2013). Deflection Of Reinforced Concrete Half-Slab. International Journal of Construction Technology and Management, 1(1), 6–12.

[34] Irawan, D., Habieb, A. B., Iranata, D., Suprobo, P., & Raka, I. G. P. (2024). Experimental Study of Two-way Half Slab Precast Concrete using Rextangular Rigid Connection. Civil Engineering Dimension, 26(1), 63–70. doi:10.9744/ced.26.1.63-70.

[35] Supriyadi, B., Siswosukarto, S., & Effi, C. P. Y. P. (2017). The Behavior Semi-precast Slab under Dynamic Load. Procedia Engineering, 171, 1204–1213. doi:10.1016/j.proeng.2017.01.488.

[36] Hillebrand, M., & Hegger, J. (2023). Shear and interface shear of semi-precast slabs with lattice girders under monotonic loading. Structural Concrete, 24(2), 3055–3076. doi:10.1002/suco.202200423.

[37] Murtadho, M. (2017). Flexural Strength Analysis of Semi-French Curved Tile Flooring System. Ph.D. Thesis, Riau University, Pekanbaru, Indonesia. (In Indonesian).

[38] Saheed, S., Aziz, F. N. A. A., Amran, M., Vatin, N., Fediuk, R., Ozbakkaloglu, T., Murali, G., & Mosaberpanah, M. A. (2020). Structural performance of shear loaded precast EPS-foam concrete half-shaped slabs. Sustainability (Switzerland), 12(22), 1-17. doi:10.3390/su12229679.

[39] Yun, Y., Jiang, J., & Chen, P. (2022). Flexural Behavior of Lattice Girder Slabs with Different Connections: Experimental Study. Advances in Civil Engineering, 2022(1). doi:10.1155/2022/7722668.

[40] Zajac, J., Drobiec, Ł., Jasiński, R., Wieczorek, M., Mazur, W., Grzyb, K., & Kisiołek, A. (2021). The behaviour of half-slabs and hollow-core slab in four-edge supported conditions. Applied Sciences (Switzerland), 11(21), 10354. doi:10.3390/app112110354.

[41] Cao, T. A., Nguyen, M. T., Pham, T. H., & Nguyen, D. N. (2023). Experimental Study on Flexural Behavior of RC–UHPC Slabs with EPS Lightweight Concrete Core. Buildings, 13(6), 1372. doi:10.3390/buildings13061372.

[42] Kim. (2015). Crack Width Control on Concrete Slab using Half-Depth Precast Panels with Loop Joints. Journal of the Korean Society of Civil Engineers, 35(1), 19. doi:10.12652/ksce.2015.35.1.0019.

[43] Szydlowski, R., & Szreniawa, M. (2017). New Concept of Semi-precast Concrete Slab on Pre-tensioned Boards. IOP Conference Series: Materials Science and Engineering, 245, 022090. doi:10.1088/1757-899x/245/2/022090.

[44] Bozzo, L. M., & Torres, Ll. (2004). A proposed semi-prefabricated prestressed composite slab. Proceedings of the Institution of Civil Engineers - Structures and Buildings, 157(5), 309–317. doi:10.1680/stbu.157.5.309.46673.

[45] Hassan, M. K., Subramanian, K. B., Saha, S., & Sheikh, M. N. (2021). Behaviour of prefabricated steel-concrete composite slabs with a novel interlocking system–Numerical analysis. Engineering Structures, 245, 112905. doi:10.1016/j.engstruct.2021.112905.

[46] Ha, S. S., Kim, S. H., Lee, M. S., & Moon, J. H. (2014). Performance evaluation of semi precast concrete beam-column connections with U-shaped strands. Advances in Structural Engineering, 17(11), 1585–1600. doi:10.1260/1369-4332.17.11.1585.

[47] Mokhtar, R., Ibrahim, Z., Jumaat, M. Z., Abd. Hamid, Z., & Abdul Rahim, A. H. (2020). Behaviour of semi-rigid precast beam-to-column connection determined using static and reversible load tests. Measurement: Journal of the International Measurement Confederation, 164, 108007. doi:10.1016/j.measurement.2020.108007.

[48] ACI Committee 211. (1996). Standard Practice for Selecting Proportions for Normal, Heavyweight, and Mass Concrete. American Concrete Institute (ACI), Farmington Hills, United States.

[49] ASTM C143/C143M-20. (2015). Standard Test Method for Slump of Hydraulic-Cement Concrete. ASTM International, Pennsylvania, United States. doi:10.1520/C0143_C0143M-20.

[50] BS EN 12390-3:2019-TC. (2019). Testing Hardened Concrete. Compressive Strength of Test Specimens. British Standards Institution (BSI), London, United Kingdom.

[51] ASTM C150/C150M-19. (2019). Standard Specification for Portland Cement. ASTM International, Pennsylvania, United States. doi:10.1520/C0150_C0150M-19.

[52] ASTM C33/C33M-23. (2024). Standard Specification for Concrete Aggregates. ASTM International, Pennsylvania, United States. doi:10.1520/C0033_C0033M-23.

[53] ASTM A615/A615M-24. (2024). Standard Specification for Deformed and Plain Carbon-Steel Bars for Concrete Reinforcement. ASTM International, Pennsylvania, United States. doi:10.1520/A0615_A0615M-24.

[54] Liu, Y. L., Huang, J. Q., Chong, X., & Ye, X. G. (2021). Experimental investigation on flexural performance of semi-precast reinforced concrete one-way slab with joint. Structural Concrete, 22(4), 2243–2257. doi:10.1002/suco.202000676.

[55] Dakhil, A. J., & Shuber, M. A. (2024). Flexural Performance of Reinforced Concrete Beams with Openings Strengthened by Varying Thickness Steel Tubes. Annales de Chimie: Science Des Materiaux, 48(1), 17–25. doi:10.18280/acsm.480103.

[56] Alahdal, A. (2024). In-plane Cyclic Response of Flexural-Dominated Partially Grouted Reinforced Masonry Shear Walls with Boundary Elements. PhD Thesis, Concordia University, Montreal, Canada.

[57] Mahmoud, M. R. I., Wang, X., Altayeb, M., Al-Shami, H. A. M., Ali, Y. M. S., & Moussa, A. M. A. (2024). Experimental and numerical study of the flexural behaviour of semi-precast slab reinforced with prestressed FRP bars. Structures, 62, 106197. doi:10.1016/j.istruc.2024.106197.

[58] Naser, K. Z., Almayah, A. A., & Abbas, A. M. (2025). Shear strength and behavior of eco-friendly RC corbels. Results in Engineering, 25, 104101. doi:10.1016/j.rineng.2025.104101.

[59] Ojaimi, M. F., Alabdulhady, M. Y., & Naser, K. Z. (2024). Influence of Concrete Compressive Strength on CFRP Strengthening and Repairing of RC Two-Way Slabs. Journal of Engineering (United Kingdom), 2024(1), 2166919. doi:10.1155/2024/2166919.

[60] Türer, A., Mercimek, Ö., Anıl, Ö., & Erbaş, Y. (2023). Experimental and numerical investigation of punching behavior of two-way RC slab with different opening locations and sizes strengthened with CFRP strip. Structures, 49, 918–942. doi:10.1016/j.istruc.2023.01.157.

[61] Ewees, M. H., Gabr, A. S. A., & Farrag, M. R. (2024). Effect of tension and compression flexural reinforcement on punching shear strength of reinforced concrete flat slab. Alexandria Engineering Journal, 99, 282–302. doi:10.1016/j.aej.2024.05.019.

[62] Said, M., Mahmoud, A. A., & Salah, A. (2020). Performance of reinforced concrete slabs under punching loads. Materials and Structures/Materiaux et Constructions, 53(4), 68. doi:10.1617/s11527-020-01509-5.

[63] Ismail El-kassas, A., Ali Bashandy, A., Mohamed Eied, F. A., & Abd El-Salam Arab, M. (2022). Effect of fibers type on the behavior of fibrous high-strength self-compacted reinforced concrete flat slabs in punching with and without shear reinforcement. Construction and Building Materials, 360, 129625. doi:10.1016/j.conbuildmat.2022.129625.

[64] International Federation for Structural Concrete (fib). (2013). fib Model Code for Concrete Structures 2010. John Wiley & Sons, Hoboken, United States. doi:10.1002/9783433604090.

[65] EN 1992-1-1 (2004) Eurocode 2: Design of concrete structures - Part 1-1: General rules and rules for buildings. European Committee for Standardization, Brussels, Belgium.